Research Article

Martin Rochette*

Design and fabrication of nonlinear optical waveguides for far-detuned wavelength conversion to the mid-infrared

https://doi.org/10.1515/aot-2018-0024
Received April 26, 2018; accepted July 18, 2018; previously published online August 11, 2018

Abstract: Highly nonlinear gain media that are optically pumped by rare-earth doped sources have become a promising approach for the fabrication of all-fiber mid-infrared laser sources. This article focuses on the recent progresses of highly nonlinear chalcogenide microwires as practical gain media for far-detuned wavelength conversion towards the mid-infrared.

Keywords: fiber optics amplifiers and oscillators; infrared; mid-infrared lasers; nonlinear optics; wavelength conversion devices.

OCIS codes: 040.3060 infrared; 060.2320 fiber optics amplifiers and oscillators; 060.4370 nonlinear optics, fibers; 130.7405 wavelength conversion devices.

1 Introduction

The spectral region of the mid-infrared (MIR) comprised in the range of 2–10 μm is of high technological interest because most molecules exhibit fundamental vibrational absorption bands, leaving distinctive spectral fingerprints which are critical for applications such as biomedical science, environmental and industrial applications, defense and security [1–4]. All-fiber optical sources that emit in the MIR are most desirable, first because of their emission in the MIR but also because all-fiber sources are intrinsically robust, and their operation is stable over time.

***Corresponding author: Martin Rochette,** Department of Electrical and Computer Engineering, McGill University, Montréal (QC) H3A 2A7, Canada, e-mail: martin.rochette@mcgill.ca

www.degruyter.com/aot

The fabrication of optical fiber sources stands on the availability of gain media. Historically, practical gain sources in optical fibers have been provided from resonant electronic transition of rare-earth ions such as e.g. Er, Yb, and Tm, making the building blocks of many fiber amplifiers and lasers as we know them today. Rare-earth doped ions in silica fibers are a most preferred source of gain for fiber lasers and fiber amplifiers because of their efficient energy conversion and good solubility in a host of silica glass. Overall, the use of various rare-earth ions has provided gain over limited bands that altogether cover the 1.0–2.0 μm spectral range [1] and [2]. At wavelengths beyond 2.0 μm, silica glass becomes unpractically opaque to optical transmission and thus MIR compatible materials such as chalcogenide and fluoride glasses have instead been considered. Although rare-earth ions offer several transitions in the MIR, chalcogenide glass hosts have yet to demonstrate lasing in the MIR [5]. Laser operation has been demonstrated at wavelengths of 2.8–2.9 μm and 3.5 μm in fluoride glass fibers embedded in free-space resonant cavities [6–10].

In this article, we demonstrate that far-detuned wavelength conversion from four-wave mixing (FWM) is a promising approach to extend the emission of rare-earth lasers further in the MIR. We compare a few highly nonlinear gain media in view of their implementation as practical amplifiers and laser sources in the MIR. We set an emphasis on chalcogenide microwires as an example of promising nonlinear medium for far-detuned wavelength conversion and provide experimental evidence of successful far-detuned wavelength conversion.

2 Highly nonlinear waveguides

Highly nonlinear waveguides are raising a lot of interest for their use in nonlinear devices such as supercontinuum sources, gain media, and wavelength converters [11]. Nonlinear waveguides are characterised by their waveguide nonlinearity parameter $\gamma \cong 2\pi n_2/\lambda A$, where n_2 is the material nonlinearity, λ is the signal wavelength, and A is the mode

effective area [11, 12]. In such devices, the nonlinear effect cumulates following a phase-shift $\phi_{NL}=\gamma P L_{\text{eff}}$, where P is the input optical power and $L_{\text{eff}}=(1-e^{-\alpha L})/\alpha$ is the effective fiber length, including the attenuation coefficient α and physical length L. The most desirable property of highly nonlinear waveguides is a waveguide nonlinearity parameter that is maximised to reduce both the required waveguide length and required peak pulse power. Such waveguides improve the device compactness and reduce the power consumption. A logical approach to maximise the waveguide nonlinearity parameter is to build the nonlinear waveguide out of a material with maximised material nonlinearity (n_2) as well as to ensure that the guided mode is strongly confined with minimised modal effective area (A).

For the interest of the discussion, materials under consideration include glasses such as SiO_2, TeO_2, Bi_2O_3, As_2S_3, and As_2Se_3 [13–19]. Although SiO_2 is not considered as a MIR-compatible material, this widespread glass and especially under the form of an SMF-28 waveguide has been preserved in the list for sake of comparison. Table 1 shows each glass considered and lists properties that will be discussed next. The first property is the upper limit in MIR wavelength transparency that must be compatible with target operation wavelengths.

Another important property of interest for the design of a highly nonlinear waveguide is the material nonlinearity, which should ideally be as large as can be, for compactness and low power consumption of the nonlinear device. It has been known since the 1970s that there is an empirical relationship in between a material's refractive indices n and n_2 [20] and [21]. Table 1 lists the measured refractive indices and measured nonlinear refractive indices of every material under consideration.

In addition to a large nonlinear coefficient, maximizing the nonlinear waveguide coefficient also involves minimizing the modal surface area of the waveguide, and thus single-mode waveguides with a large core to cladding refractive index contrast are required. Optical microwires and suspended core fibers use this approach [22–29]. In both cases, the core and cladding of the waveguide are made of two distinct materials. The cladding of the microwire consists of a material that differs from the material of the core (e.g. glass, polymer, air) whereas for the suspended core fiber, the low refractive index material that forms the cladding is air in general. An advantage of the microwire over the suspended core fiber is the low insertion losses to this waveguide in a taper configuration.

The nonlinear waveguide parameter in a case of high modal confinement is precisely evaluated using a vectorial analysis approach that considers the modal field distribution [30]. Figure 1A shows the nonlinear waveguide parameter at a wavelength of 2.0 μm as a

Table 1: Materials under investigation and their properties at a wavelength of 2 μm when in the form of optical wires surrounded by air, at the exception of the silica standard single-mode fiber (SMF-28) used as a reference.

	MIR (μm)	n (–)	n_2 (m²/W)	γ_{max} (rad/W-m)	$A_{eff,min}$ (μm²)	L_{eff} (m)	$\gamma_{max}L_{eff}$ (rad/W)	P_0 @ 40 dB, 0.1 m (W)
SiO_2 (SMF-28)	2	1.44	3.1×10^{-20}	10^{-3}	85	10	0.01	53 k
TeO_2	5	2.00	2.5×10^{-19}	2.7	0.64	2.4	6	20
Bi_2O_3	3	2.02	3.2×10^{-19}	3.6	0.70	5.4	19	15
As_2S_3	9	2.43	2.7×10^{-18}	27	0.36	7.2	194	2.0
As_2Se_3	12	2.81	8.4×10^{-18}	154	0.24	4.8	739	0.34

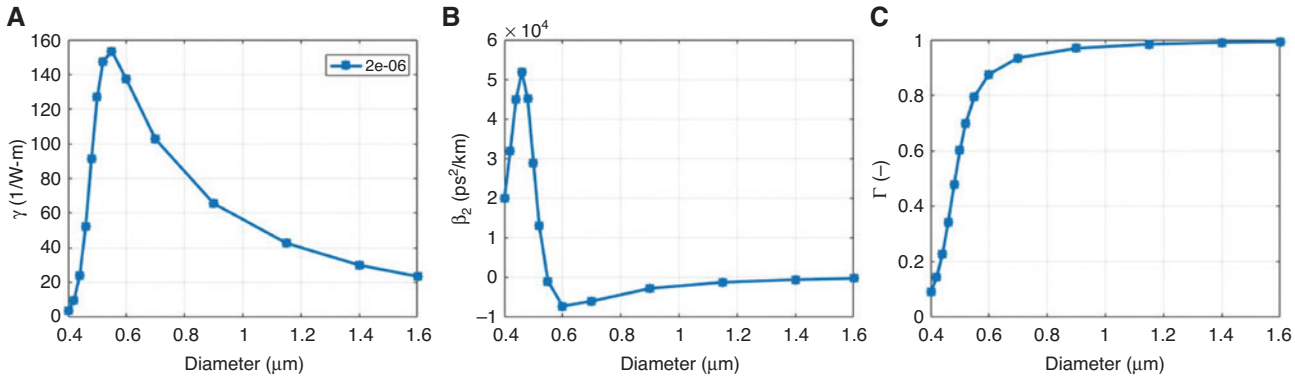

Figure 1: Optical parameters of the fundamental mode in a As_2Se_3 wire surrounded by air at a wavelength of 2.0 μm. (A) Group-velocity dispersion. (B) Nonlinear waveguide parameter. (C) Modal confinement.

function of diameter for an As_2Se_3 wire surrounded by air. Strong modal confinement in a high refractive index contrast wire occurs when the wire diameter is near the operation wavelength, in the example of Figure 1 that is $d \cong \lambda/n = 0.7$ μm. The nonlinear waveguide parameter reaches a maximum of $\gamma_{max} = 154$ rad/W-m at $d = 0.58$ μm and abruptly decreases for smaller diameters due to the mode size that increasingly exceeds the wire diameter, and thus having an increasingly larger fraction of the mode energy that lies outside the wire. For wire diameters increasing from $d = 0.58$ μm, the nonlinear waveguide parameter decreases gradually because of the decreased modal confinement.

Determination of the modal solutions of a high refractive index contrast waveguide is performed from solving a standard characteristic waveguide equation [31]. From the modal solutions, it is most interesting to extract values of group-velocity dispersion (β_2) and confinement factor. Figure 1B shows the group-velocity parameter as a function of diameter of an As_2Se_3 wire at a wavelength of 2.0 μm. Although the material dispersion of As_2Se_3 is 700 ps²/km at a wavelength of 2.0 μm, when the wire diameter is in the order of the wavelength ($d \cong 0.7$ μm), optical confinement influences greatly the total dispersion that becomes strongly increased or decreased relative to material dispersion. This variation in total chromatic dispersion is caused by the sole effect of waveguide dispersion, and it is also generalised for any high refractive index contrast waveguide. This thus enables a given nonlinear waveguide to be used in various levels of chromatic dispersion. Figure 1C show the confinement factor, defined as the ratio of modal energy contained in the core to the total mode energy, as a function of the As_2Se_3 wire diameter. For a diameter in the order of the wavelength $d \cong 0.7$ μm, the confinement factor is strong with $\Gamma = 0.97$, but it decreases abruptly for decreasing wire diameters, an indication that the mode cannot be confined any tighter.

The analysis of γ as a function of wire diameter has been performed for all materials of Table 1 and their resulting γ_{max} is noted into Table 1, at the exception of SMF-28 which is considered in a usual weakly guiding geometry, for reference. The effective modal area (A_{eff}) is another parameter of interest that is included in Table 1. Under a variable wire diameter, A_{eff} reaches a minimum at the same diameter than γ_{max}. This value of A_{eff}, noted $A_{eff,min}$, is also added into Table 1.

Nonlinear waveguides with strong γ may seem to have a relative advantage over those with lower γ for the generation of nonlinear gain. However, the nonlinear gain depends not only on γ but also on the length over which nonlinear interaction occurs. In this context, a lossy material may turn out to be disadvantaged with respect to another one, even though having a large γ. A good figure of merit to classify lossy waveguides then turns out to be a normalised nonlinear phase-shift per unit of pump power or following definitions above, $\phi_{NL}/P = \gamma L_{eff}$, where L_{eff} includes waveguide losses. The product $\gamma_{max} L_{eff}$ has been added in Table 1 for every material considered. An intrinsically highly nonlinear and low-loss material like As_2Se_3 under the form of a strongly confining wire waveguide is a suitable candidate for an efficient generation of nonlinear gain in the MIR. Hybrid microwires made of an As_2Se_3 core and cladding of different material such as As_2S_3, PMMA, COP, and CYTOP, have been fabricated to replace air-cladded microwires [32, 33]. Microwires cladded with a solid material have better mechanical robustness than air-cladded microwires, and thus represent a good practical alternative.

3 Nonlinear gain

In a quest for all-optical fiber sources in the MIR, knowing that gain from rare-earth doped fibers is available up to 2.0 μm and might be available at a few specific wavelengths in the 2.0–3.5 μm wavelength range, the use of nonlinear gain is desirable to fill the many uncovered gaps of the 2.0–3.5 μm wavelength range as well as to cover wavelengths >3.5 μm. Wavelength conversion generated from Raman shifting of solitons enables far-detuning but has limited detuning caused by the nature of the process that consists in cascaded wavelength increments along the nonlinear waveguide [34] and [35]. The most promising source of nonlinear gain arises from FWM as it has the potential for wavelength conversion far-detuned from the pump by several tens of THz [36]. Of interest is gain provided by modulation instability (MI) of a pump in a well-designed nonlinear medium [37–39].

Figure 2A shows the generation of a Stokes and Anti-Stokes sidebands resulting from MI of a pump signal. In this process, a pair of photons from the pump is converted into one Stokes photon and one anti-Stokes photon. The wavelength of the sidelobes relative to the pump is determined by phase-matching conditions of the parametric process, with highest occupation probability where phase mismatch is zero and decreasing occupation probability with increasing phase mismatch. In practice, this appear as sideband gain profiles following $G_s = 1 + (\gamma P/g)^2 \sinh^2(gL_{eff})$ where $g = \sqrt{(\gamma P)^2 - (\kappa/2)^2}$ is the gain coefficient, $\kappa = 2\gamma P + 2\sum_{m=1}^{\infty} \beta_{2m} (\Delta\omega)^{2m}/(2m)!$ is the phase mismatch

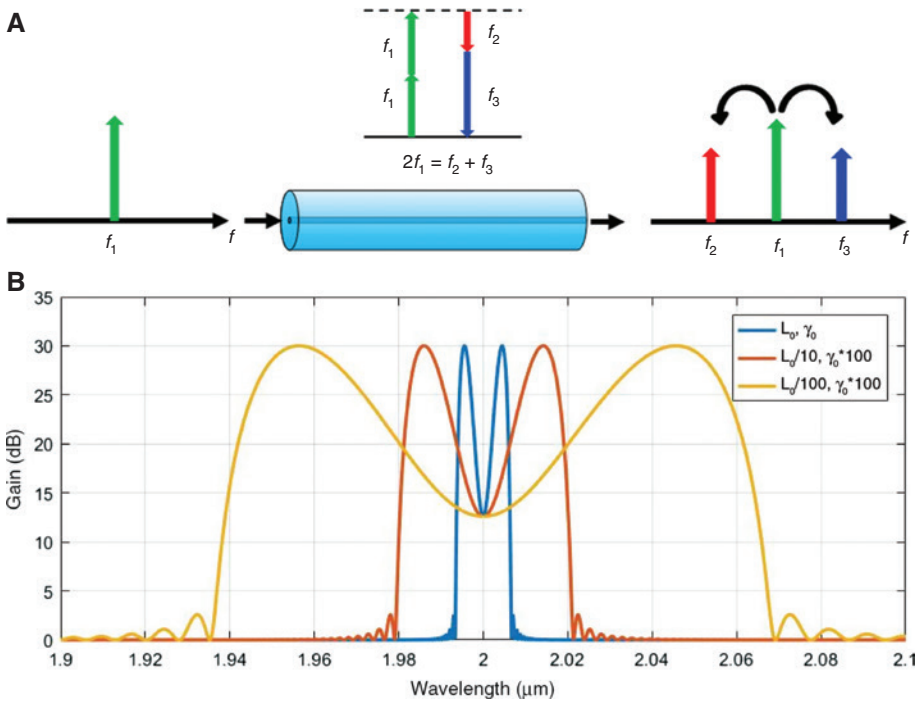

Figure 2: (A) Modulation instability of a pump generates Stokes and anti-Stokes sidelobes. (B) Typical gain spectra from modulation instability of a pump at a wavelength of 2.0 μm and power P_0 (pump not shown). The media considered have identical figure of merit $\phi_{NL}/P_0 = \gamma_0 L_0$, leading to identical maximum gain but gain bandwidth increasing proportionally with $1/\sqrt{L_{\text{eff}}}$.

parameter, $\beta_n = d^n\beta/d\omega^n$ are derivatives of the phase constant evaluated at the pump wavelength, and $\Delta\omega$ is the angular frequency coordinate relative to the pump frequency [36]. Figure 2B shows typical gain distributions from a pump at a wavelength of 2 μm (pump not shown) and close to the zero-dispersion wavelength of the waveguide. Three plots are shown with equal amount of accumulated nonlinearity ϕ_{NL}, but with variable lengths of nonlinear media. From these plots, it is interesting to notice that the maximum unsaturated gain $G_{s,\max} = 0.25\exp(2\gamma P L_{\text{eff}}) = 0.25\exp(2\phi_{NL})$ depends solely on ϕ_{NL}, when $\phi_{NL} \gg 1$. This maximum is found at the spectral frequency of perfect phase-matching, or $\kappa = 0$. A second observation of Figure 2B that has an important impact on the design of nonlinear media is that the gain bandwidth covered by FWM increases proportionally with $1/\sqrt{L_{\text{eff}}} = \sqrt{\gamma P/\phi_{NL}}$. When comparing various nonlinear media that have equivalent γL_{eff} and considered as black boxes into which is injected equal amount of power, the nonlinear medium with the largest γ will be the one advantageously allowing the largest gain bandwidth. This strengthen the interest of designing nonlinear media with γ as large as can be, in order to access a spectrally broad FWM gain around the gain maximum.

To enable far-detuned wavelength conversion, perfect phase-matching must occur spectrally far from the pump wavelength. A successful approach to this involves reaching $\kappa = 0$ from a balance of β_2 just slightly normal ($\beta_2 > 0$) and β_4 negative. Looking at the components that make the phase-mismatch parameter, the nonlinear phase-shift expressed by $2\gamma P$ is always positive. Combining this with a slightly positive $\beta_2(\Delta\omega)^2$ and negative $\beta_4(\Delta\omega)^4$ component eventually brings κ down to zero when $\Delta\omega$ is large enough for $\beta_4(\Delta\omega)^4$ to become significant. As shown in Figure 1B, values of β_2 close to zero conveniently occur at wire diameters that also lead to strong γ. This has an important practical impact for the fabrication of far-detuned wavelength converters from microwires.

A proper engineering of wire diameter from a known pump wavelength is key for the fabrication of far-detuned wavelength converters. Figure 3A shows expected gain spectra of a 10 cm long As_2Se_3 microwire coated with CYTOP and using a pump with a power of 10 W at a wavelength of 2 μm. Spectra are shown for wire diameters ranging 1.3–1.8 μm by steps of 0.1 μm. The wire diameter clearly impacts chromatic dispersion parameters and in return leads to various phase-matching conditions, enabling the adjustment of the wavelength at which $G_{s,\max}$ occurs. Figure 3B shows the experimental measurement of spontaneous emission resulting from MI in an As_2Se_3 microwire coated with CYTOP [32]. The wire diameter and length are 1.63 μm and 10 cm. The pump laser has a wavelength

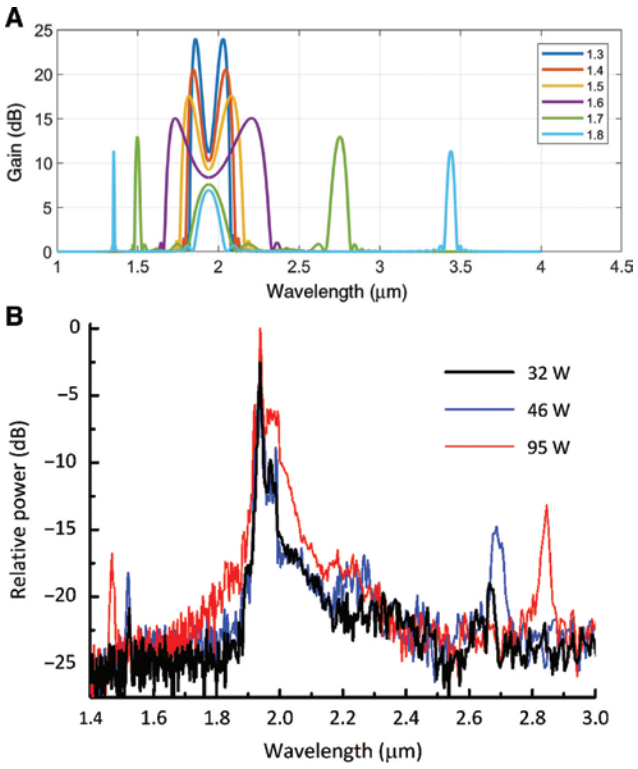

Figure 3: (A) Theoretical gain spectra from modulation instability of 10 cm long As_2Se_3 wires coated with CYTOP. The different spectra correspond to different wire diameters in the 1.3–1.8 μm range. Pump wavelength is 2 μm (not shown) with a power of 10 W. (B) Spontaneous emission spectra of a 1.94 μm wavelength pump experiencing modulation instability after propagation in a 10 cm long As_2Se_3 wire coated with CYTOP. Wire diameter is 1.63 μm and pump power is varied in a range of 32–95 W, tuning the sidelobes.

of 1.94 μm and variable power ranging 32–95 W. MI leads to sidelobes clearly identified in the 2.65–2.85 μm range and correspond to spontaneous emission from the gain generated by FWM. Wavelength detuning resulting from this experiment is ~0.95 μm (~49 THz) and has potential to be increased with further designs and experiments. The generated sidelobe can be wavelength-tuned by adjustment of the pump wavelength and/or power. Currently observed with a relatively low power resulting from spontaneous emission, it is expected that the inclusion of such a microwire inside a resonant cavity will strongly improve power conversion via parametric oscillation [40] and [41].

4 Conclusion

The ability of a waveguide to generate nonlinearity is maximised by the careful combination of a highly nonlinear material with a waveguide geometry that strongly confines the propagating mode. We compared different waveguide geometries and compositions, leading to an indication that chalcogenide microwires have a strong potential for MIR wavelength conversion. Chalcogenide microwires are compatible with far-detuned wavelength conversion in the MIR, resulting in several tens of THz of wavelength detuning.

Funder: Natural Sciences and Engineering Research Council of Canada, Funder Id: 10.13039/501100000038, Grant Number: Discovery grants.

References

[1] M. Pollnau and S. D. Jackson, in 'Solid-state Mid Infrared Sources', Ed. By I. T. Sorokina and K. L. Vodopyanov (Springer, New York, 2003) pp. 225–261.
[2] F. K. Tittel, D. Richter and A. Fried, in 'Solid-state Mid Infrared Sources', Ed. By I. T. Sorokina and K. L. Vodopyanov (Springer, New York, 2003) pp. 458–529.
[3] Y. Yu, X. Gai, T. Wang, P. Ma, R. Wang, et al., Opt. Mater. Express 3, 1075–1086 (2013).
[4] M. Kumar, M. N. Islam, F. L. Terry, M. J. Freeman, A. Chan, et al., Appl. Opt. 51, 2794–2807 (2012).
[5] A. B. Seddon, Z. Tang, D. Furniss, S. Sujecki and T. M. Benson, Opt. Express 18, 26704–26719 (2010).
[6] P. Zhou, X. Wang, Y. Ma, H. Lü and Z. Liu, Laser Phys. 22, 1744–1751 (2012).
[7] T. Hu, S. D. Jackson and D. D. Hudson, Opt. Lett. 40, 4226–4228 (2015).
[8] S. Duval, J.-C. Gauthier, L.-R. Robichaud, P. Paradis, M. Olivier, et al., Opt. Lett. 41, 5294–5297 (2016).
[9] O. Henderson-Sapir, J. Munch and D. J. Ottaway, Opt. Lett. 39, 493–496 (2014).
[10] R. I. Woodward, D. D. Hudson, A. Fuerbach and S. D. Jackson, Opt. Lett. 42, 4893–4896 (2017).
[11] G. P. Agrawal, Nonlinear Fiber Optics, 5th edition (Academic press, Oxford, 2013).
[12] V. Tzolov, M. Fontaine, N. Godbout and S. Lacroix, J. Opt. Soc. Am. B 12, 1933–1941 (1995).
[13] B. J. Eggleton, B. Luther-Davies and K. Richardson, Nat. Photonics 5, 141 (2011).
[14] A. Zakery and S. R. Elliott, J. Non-Cryst. Solids 330, 1–12 (2003).
[15] R. E. Slusher, G. Lenz, J. Hodelin, J. Sanghera, L. Brandon Shaw, et al., J. Opt. Soc. Am. B 21, 1146 (2004).
[16] Z. Chen, A. J. Taylor and A. Efimov, Opt. Express. 17, 5852–5860 (2009).
[17] J. H. Lee, T. Nagashima, T. Hasegawa, S. Ohara, N. Sugimoto, et al., J. Light. Technol. 24, 22–28 (2006).
[18] A. Lin, A. Zhang, E. J. Bushong and J. Toulouse, Opt. Express 17, 16716–16721 (2009).
[19] P. Domachuk, N. A. Wolchover, M. Cronin-Golomb, A. Wang, A. K. George, et al., Opt. Express 16, 7161–7168 (2008).
[20] C. C. Wang, Phy. Rev. B 2, 2045–2048 (1970).
[21] J. H. V. Price, T. M. Monro, H. Ebendorf-Heidepreim, F. Poletti, P. Horak, et al., J. Sel. Topics Quant. Electron. 13, 738–749 (2007).

[22] P. Dumais, F. Gonthier, S. Lacroix, J. Bures, A. Villeneuve, et al., Opt. Lett. 18, 1996–1998 (1993).
[23] M. A. Foster, A. C. Turner, M. Lipson and A. L. Gaeta, Opt. Express 16, 1300–1320 (2008).
[24] E. C. Magi, L. B. Fu, H. C. Nguyen, M. R. Lamont, D. I. Yeom, et al., Opt. Express 15, 10324–10329 (2007).
[25] C. Baker and M. Rochette, Opt. Express 18, 12391–12398 (2010).
[26] C. Baker and M. Rochette, IEEE Photon. J. 4, 960–969 (2012).
[27] J. H. Lee, Z. Yusoff, W. Belardi, M. Ibsen, T. M. Monro, et al., IEEE Photon. Technol. Lett. 15(3), 440–442 (2003).
[28] P. Russell, Science 299, 358–362 (2003).
[29] P. Petropoulos, H. Ebendorff-Heidepriem, V. Finazzi, R. C. Moore, K. Frampton, et al., Opt. Express 11, 3568–3572 (2003).
[30] S. Afshar and T. M. Monro, Opt. Express 17, 2298–2318 (2009).
[31] K. Okamoto, Fundamentals of Optical Waveguides, second edition (Academic Press, Oxford, 2006).
[32] L. Li, N. Abdukerim and M. Rochette, Opt. Express 24, 18931–18937 (2016).
[33] L. Li, A. Al Kadry, N. Abdukerim and M. Rochette, Opt. Mat. Express 6, 912–921 (2016).
[34] A. Al Kadry and M. Rochette, J. Light. Technol. 31, 1462–1467 (2013).
[35] A. Al Kadry and M. Rochette, J. Opt. Soc. Am. B 29, 1347–1355 (2012).
[36] M. E. Marhic, Fiber Optical Parametric Amplifiers, Oscillators and Related Devices (2008 Cambridge Press, Cambridge).
[37] R. Ahmad and M. Rochette, Opt. Express 20, 9572–9580 (2012).
[38] T. Godin, Y. Combes, R. Ahmad, M. Rochette, T. Sylvestre, et al., Opt. Lett. 39, 1885–1888 (2014).
[39] L. Li, N. Abdukerim and M. Rochette, Opt. Lett. 42, 639–642 (2017).
[40] N. Abdukerim, L. Li and M. Rochette, Opt. Lett. 41, 4364–4367 (2016).
[41] R. Ahmad and M. Rochette, Opt. Express 20, 10095–10099 (2012).